

## ATMOSPHERIC, CLIMATIC, AND ECOLOGICAL CONTROLS ON EXTREME WILDFIRE YEARS IN THE NORTHWESTERN UNITED STATES

ZE'EV GEDALOF,<sup>1,3</sup> DAVID L. PETERSON,<sup>2</sup> AND NATHAN J. MANTUA<sup>1</sup>

<sup>1</sup>*Climate Impacts Group, Center for Science in the Earth System, Joint Institute for the Study of the Atmosphere and Ocean, University of Washington, Box 354235, Seattle, Washington 98195-4235 USA*

<sup>2</sup>*USDA Forest Service, Pacific Northwest Research Station, Fire and Environmental Research Applications Team, 400 N 34th Street, Suite 201, Seattle, Washington 98103 USA*

**Abstract.** Wildland fire is an important disturbance agent in forests of the American Northwest. Historical fire suppression efforts have contributed to an accumulation of fuels in many Northwestern forests and may result in more frequent and/or more severe wildfire events. Here we investigate the extent to which atmospheric and climatic variability may contribute to variability in annual area burned on 20 National Forests in Washington, Oregon, and Idaho. Empirical orthogonal function (EOF) analysis was used to identify coherent patterns in area burned by wildfire in the Pacific Northwest. Anomaly fields of 500-hPa height were regressed onto the resulting principal-component time series to identify the patterns in atmospheric circulation that are associated with variability in area burned by wildfire. Additionally, cross-correlation functions were calculated for the Palmer drought severity index (PDSI) over the year preceding the wildfire season. Parallel analyses based on superposed epoch analysis focused only on the extreme fire years (both large and small) to discriminate the controls on extreme years from the linear responses identified in the regression analyses. Four distinct patterns in area burned were identified, each associated with distinct climatic processes. Extreme wildfire years are forced at least in part by antecedent drought and summertime blocking in the 500-hPa height field. However the response to these forcings is modulated by the ecology of the dominant forest. In more mesic forest types antecedent drought is a necessary precondition for forests to burn, but it is not a good predictor of area burned due to the rarity of subsequent ignition. At especially dry locations, summertime blocking events can lead to increases in area burned even in the absence of antecedent drought. At particularly xeric locations summertime cyclones can also lead to increased area burned, probably due to dry lightning storms that bring ignition and strong winds but little precipitation. These results suggest that fuels treatments alone may not be effective at reducing area burned under extreme climatic conditions and furthermore that anthropogenic climate change may have important implications for forest management.

**Key words:** climatic variability; empirical orthogonal function analysis; Pacific Decadal Oscillation; Pacific Northwest; top-down controls; wildfire.

### INTRODUCTION

There is a growing recognition that fire plays an integral role in developing the structure and composition of forest ecosystems in the Pacific Northwest (Agee and Huff 1987, Cwynar 1987, Huff 1995, Lertzman et al. 1998, Taylor and Skinner 1998, Everett et al. 2000). Historical fire exclusion practices are being revised to reflect these changes in attitude; forests are now subjected to “fire management” rather than the default suppression and exclusion policies of the past. Naturally occurring fires are occasionally allowed to burn, prescribed fires are intentionally set, and fuels

are managed to encourage natural fire regimes (Agee 1993). Fire exclusion continues at locations where cultural, economic, or ecological values require it. The exclusion of fire over the last century has significantly modified the structure and composition of Northwestern forests (Hessburg et al. 2000) and made many types of forest more prone to extreme fire events (Agee 1997, 1998, but see Johnson et al. [2001]). Consequently, a better understanding of the factors that contribute to severe, extensive fires is critical for the integration of fire as an ecological process into managed landscapes.

Fire behavior is determined largely by the nature of the fuels, topography, and weather occurring at the site of ignition (Johnson 1992). Of these factors weather is the most variable over time and the most poorly understood. Furthermore, a substantial proportion of total area burned is likely caused by relatively few fires that occur under extreme weather conditions (Schroeder 1969, Strauss et al. 1989, Johnson and Wowchuk 1993,

Manuscript received 21 April 2003; revised 17 May 2004; accepted 4 June 2004; final version received 28 June 2004. Corresponding Editor: M. L. Goulden.

<sup>3</sup> Present address: Department of Geography, University of Guelph, Guelph, Ontario, Canada N1G 2W1. E-mail: zgedalof@uoguelph.ca

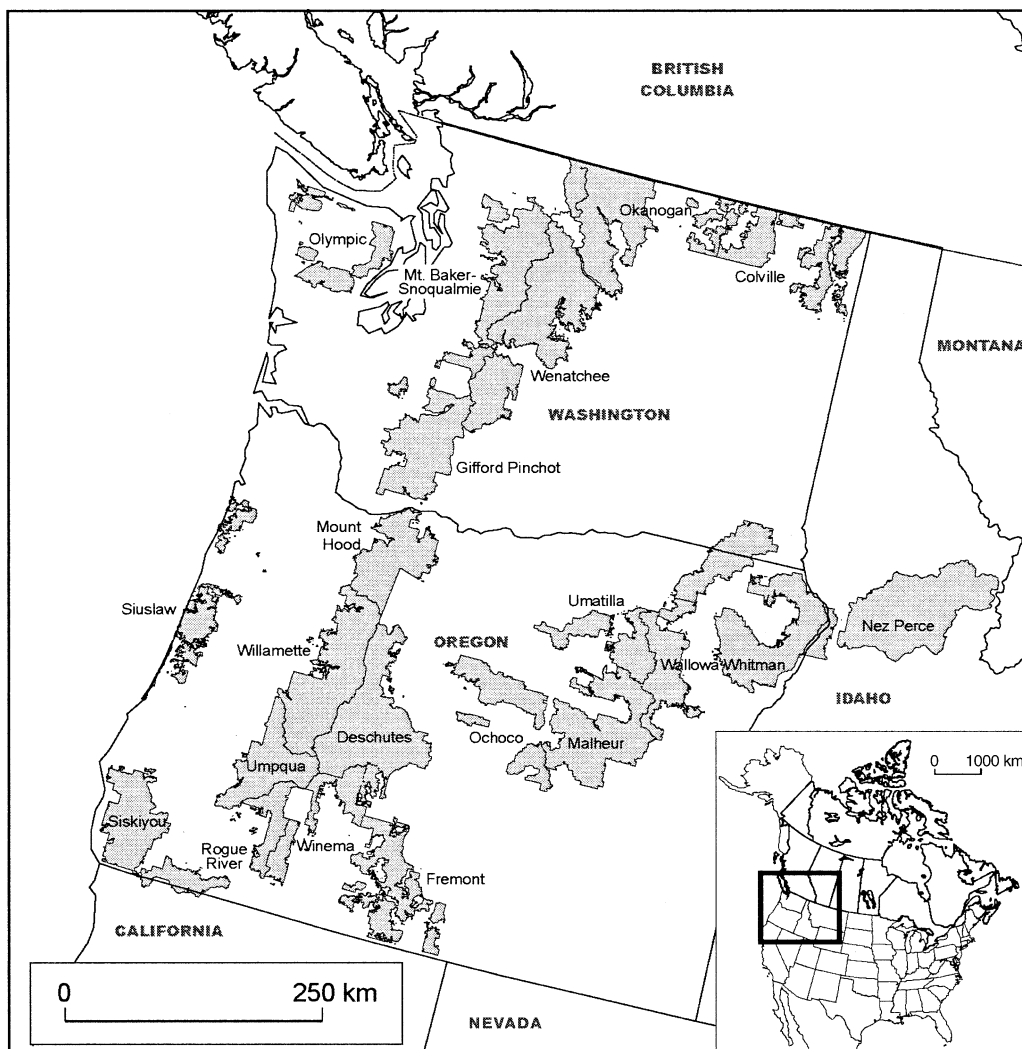


FIG. 1. Locations of the 20 National Forests in the northwestern United States considered in this analysis.

Skinner et al. 2002). The goals of this study are to determine if underlying patterns exist in annual area burned in the northwestern United States and to determine the extent to which these patterns are associated with mid-tropospheric circulation anomalies and variability in antecedent temperature, precipitation, and drought. This approach is distinct from most previous studies in two respects: (1) we do not treat the area west of the Rocky Mountains as a single coherent unit; and (2) we address large fire seasons, rather than individual large fires.

We divided the study area into multiple regions with coherent fire regimes for several reasons. First, the large contrast in forest types that occur throughout this region is almost certainly a response to different climatic and fire regimes that are in operation (Franklin and Dyrness 1973, Agee 1993). Given these differences it seems probable that there may be more than a single pattern in annual area burned, as well as distinct cli-

matic controls on these patterns. Furthermore, by focusing on extreme wildfire years rather than individual large fires we are better able to assess the role of the atmosphere in forcing wildfires. By averaging over space and time we reduce the role that individual site characteristics play in contributing to fire extent. Lastly, by identifying elements of climate that contribute to extreme wildfire years in specific regions of the American Northwest we provide fire managers with a tool that can potentially be used to anticipate the severity of the upcoming fire season.

#### REGIONAL SETTING

Twenty U.S. National Forests were considered in the analysis, located throughout Washington, Oregon, and Idaho (Fig. 1). This study region abuts the Canadian border to the North, the Pacific Ocean to the west, the Rocky Mountains to the east, and California and Nevada to the south. The Cascade Mountains unevenly

TABLE 1. Biophysical characteristics of the 20 National Forests in northwestern United States considered in this analysis.

National Forest	Dominant forest types†	Mean annual precipitation (cm)	Typical fire regime‡
Colville	<b>Douglas-fir, grand fir</b> , Engelmann spruce, subalpine fir	52	3–5
Deschutes	<b>lodgepole pine, ponderosa pine</b> , Douglas-fir, grand fir	501	1–2
Fremont	<b>ponderosa pine</b> , western juniper, lodgepole pine	67	2–3
Gifford Pinchot	<b>western hemlock, Douglas-fir</b> , Pacific silver fir, mountain hemlock	157	4–5
Malheur	<b>Douglas-fir, grand fir</b> , ponderosa pine	35	3–5
Mount Baker-Snoqualmie	<b>western hemlock, Douglas-fir, Pacific silver fir</b> , mountain hemlock	166	5–6
Mt. Hood	<b>western hemlock, Douglas-fir, grand fir</b> , mountain hemlock, subalpine fir	153	4–5
Nez Perce	<b>Douglas-fir, grand fir, ponderosa pine</b> , Engelmann spruce, subalpine fir	59	4–6
Ochoco	<b>Douglas-fir, grand fir</b> , ponderosa pine	31	3–4
Okanogan	<b>Douglas-fir</b> , western hemlock, Engelmann spruce, subalpine fir	108	3–5
Olympic	<b>Sitka spruce, western hemlock, Pacific silver fir</b> , Douglas-fir, mountain hemlock	174	5–6
Rogue River	<b>Douglas-fir, white fir, red fir</b> , ponderosa pine	71	3–5
Siskiyou	<b>Douglas-fir, western hemlock</b> , coast redwood, white fir, red fir	130	2–5
Siuslaw	<b>western hemlock, Sitka spruce, Douglas-fir, grand fir</b> , Pacific silver fir	168	4–6
Umatilla	<b>Douglas-fir, grand fir</b> , ponderosa pine, Engelmann spruce, subalpine fir	41	3–5
Umpqua	<b>Douglas-fir, ponderosa pine</b> , grand fir, incense cedar,	98	4–5
Wallowa-Whitman	<b>Douglas-fir, ponderosa pine</b> , grand fir, Engelmann spruce, subalpine fir	47	2–4
Wenatchee	<b>Douglas-fir, grand fir, ponderosa pine</b> , subalpine fir	99	2–4
Willamette	<b>Douglas-fir, incense cedar, ponderosa pine, Oregon white fir, red fir</b> , mountain hemlock	103	1–4
Winema	<b>ponderosa pine, lodgepole pine</b> , Douglas-fir, grand fir	64	1–3

† Species identified in boldface type are most commonly occurring.

‡ Fire regimes are based on Agee (1993): 1, infrequent light surface fires (&gt;25-yr return interval); 2, frequent light surface fires (1–25 yr return interval); 3, infrequent severe surface fire (&gt;25-yr return interval); 4, short return interval crown/severe surface fire (25–100 yr); 5, long return interval crown/severe surface fire (100–300 yr); 6, very long return interval crown/severe surface fire (300+ yr).

bisect the study area along a north–south axis and exert a strong orographic control on the region's climate. The Olympic and Coast Mountains, located in northwestern Washington and coastal Oregon, respectively, exert additional climatic and ecological influences on the region. Southeastern Oregon is characterized by a complex mosaic of highlands, mountainous terrain, and basin and range topography that give rise to a spatially heterogeneous landscape.

This physiographic setting influences regional fire regimes in several ways: (1) orographic controls on temperature and moisture availability give rise to characteristic vegetation assemblages that in turn influence fuel accumulation and flammability of the landscape; (2) differences in parent material influence rates of soil development and soil chemistry, which can influence the relative abundance of forest types; (3) regional topography influences the location and intensity of summertime convection cells that affect the frequency of lightning ignitions; and (4) regional differences in elevation lead to dramatic adiabatic changes in temperature and relative humidity as air masses are translocated, in particular when circulation favors anomalous easterly winds, which can dry fuels quickly and lead to especially severe wildfire hazards.

Orographic controls on precipitation lead to a considerable disparity in total annual precipitation across the study region. Mean annual precipitation ranges from over 250 cm on the Olympic Peninsula to less than 25 cm in the interior Columbia Basin. Mean precipitation west of the Cascades is ~140 cm/yr, about four times the 40-cm annual mean east of the Cascades. The distribution of mean annual temperature is less affected by the mountains than is precipitation, although coastal regions are on average ~2°C warmer than interior regions. However, the Cascade Mountains mark the approximate boundary between maritime and continental climates in the region, with summer–winter differences in temperature substantially greater east of the Cascades crest.

These differences in regional climate are reflected in the dominant vegetation types that occur throughout the Pacific Northwest (Franklin and Dyrness 1973) (Table 1). Within the study region characteristic forest types range from coastal temperate rainforest, where fire return intervals may be a millennium or longer (Fahnestock and Agee 1983, Gavin et al. 2003b), to open ponderosa pine savannah, where fires may recur more than once per decade (Weaver 1959, Bork 1984, Agee 1993, Everett et al. 2000). (The mean fire return

interval is defined here as the mean number of years between two successive fire events in a given landscape. It is most commonly applied to regions with low-severity to moderate-severity fire regimes. The terms “fire rotation” and “fire cycle” are more commonly applied to forests with moderate- to high-severity fire regimes. These latter parameters are normally estimated from age-distribution models rather than from fire scars or other direct measurements, but otherwise indicate the same fire return properties [Baker and Ehle 2001, Li 2002].) Fire regimes exhibit similar variability, with low-, moderate-, and high-severity fire regimes represented throughout the region (Franklin and Dyrness 1973, Agee 1993). The natural fire regime is strongly controlled by topographic variability (e.g., Gavin et al. 2003a), and most of the National Forests considered in this analysis are composed of stands representing a diverse range of natural fire regimes, including sites where mixed severity fires are common.

In addition to spatial variability in fuel production there is also variability in ignition frequency. Lightning strikes, the most important natural cause of fire ignitions in the Pacific Northwest, exhibit substantial spatial variability. West of the Cascade Mountains the annual density of lightning strikes is normally  $<0.05$  strikes/km<sup>2</sup>. In contrast, portions of Deschutes, Ochoco, Malheur, and Umatilla National Forests typically experience 0.25 strikes·km<sup>-2</sup>·yr<sup>-1</sup> and Fremont, Wallowa-Whitman, and Nez Perce more than 0.35 strikes·km<sup>-2</sup>·yr<sup>-1</sup>.

Regional differences in elevation contribute to the most severe types of fire weather in western North America. The continental interior is generally higher than the intermountain regions, which are in turn higher than coastal areas. Under normal conditions, air masses in the mid-troposphere move eastward from the coast to the interior, meandering through an alternating series of troughs and ridges. The Rocky Mountains contribute to the formation of a semi-permanent high-pressure ridge over western North America and a corresponding low-pressure trough over central and eastern North America. This circulation pattern can be interrupted by the development of a blocking ridge, characterized by an anomalous high-pressure system that remains quasi-stationary over the far eastern Pacific Ocean or western North America for prolonged intervals. These systems divert moisture away from the region immediately below and downstream and in some circumstances can lead to anomalous easterly winds. These “foehn” or “chinook” winds warm and dry adiabatically as they move from the relatively warm and dry high-elevation continental interior towards the coastal lowlands. Under these conditions surface temperatures increase rapidly, relative humidity can plunge, and fuels can quickly become extremely dry (Flannigan and Harrington 1988, Johnson and Wowchuk 1993, Skinner et al. 1999).

Blocking events may be interrupted by the rapid passage of one or more low-pressure systems that bring strong winds and potential ignition sources in the form of lightning (Schroeder 1969). When the blocking ridge has been especially strong and persistent, the extreme pressure gradient associated with cyclonic storms causes strong winds that result in rapidly spreading wildfires of unusual severity (Countryman et al. 1969, Sando and Haines 1972, Finklin 1973, Street and Birch 1986). Alternatively, at the edge of these high-pressure cells convective action alone can generate the winds (and ignition source) that contribute to high-severity burning conditions and rapid rates of fire spread.

#### DATA

Annual area burned by wildfire in the Pacific Northwest was determined in each of the 20 National Forests for the years 1948 to 1995, from USDA Forest Service Annual Fire Reports (W. S. Keeton, J. F. Franklin, and P. W. Mote, *unpublished manuscript*). Each year's observation was divided by the total area monitored to form a dimensionless burned area index (BAI) representing the proportion of each National Forest that burned in that year. This standardization was necessary because the area monitored for wildfire has not been consistent over time, and consequently there are spurious trends in area burned that result simply from the increase in area monitored. There are also differences in the relative sizes of the National Forests that make direct comparison otherwise difficult. The area burned data were available only as calendar-year totals, so no attempt to discriminate the timing of events within the fire season was possible. We also considered a region-wide composite BAI, defined as the area-weighted mean of annual area burned in each of the 20 National Forests. This regional chronology provides a basis for comparison to the regionalization strategy that we use, which must exhibit better coherence than this region-wide chronology in order to justify its additional complexity.

The upper-air observations consist of gridded measurements of 500-hPa geopotential height values, taken from the National Centers for Environmental Prediction/National Center for Atmospheric Research “re-analysis” project (Kalnay et al. 1996). Monthly means were used for this analysis. The spatial domain considered included the region from 90° to 180° W and from 30° to 75° N, with a resolution of 2.5° latitude by 2.5° longitude. The temperature, precipitation, and Palmer Drought Severity Index (PDSI) data were taken from the time bias-corrected state climatic divisional data set (Guttman and Quayle 1996). The divisional data are derived from area-weighted means of temperature and precipitation over regions of relatively homogeneous climate and are reported as monthly means. These data probably represent conditions in the National Forests better than single station data due to this spatial integration. All of the meteorological data had

the annual cycle removed and were converted to anomaly values prior to analysis.

One problematic issue that arises here derives from the scale mismatch between the annual index of area burned and monthly climatic parameters. Because fires can occur at any time during the fire season and because the timing of the peak fire season can vary from year to year, it is difficult to assess whether an observed association between annual BAI and a monthly climatic parameter indicates an antecedent, coeval, or spurious association. Nonetheless, there are at least four reasons to believe that insight into the causes of variability in annual area burned may be derived from analyses of monthly data: (1) The temporal scale on which mid-tropospheric blocking events operate extends from days to weeks, and seasonal means of 500-hPa anomalies or downstream teleconnections may obscure meaningful relationships. (2) Because of the relatively large sample size considered here (20 National Forests, 48 yr) it is reasonable to assume that there is some preferred seasonality inherent to the record of area burned. This assumption is supported by analyses of recent records: Westerling et al. (2003) developed a comprehensive, spatially explicit database of monthly area burned on public lands from 1980 to 2000. These data show that there is strong seasonality to wildfires in Washington, Oregon, and Idaho: 6% of annual area burned has occurred in June, 40% in July, 47% in August, and 5% in September (A. L. Westerling, *personal communication*). Approximately 1.5% of total area burned occurs in October, and less than 0.1% occurs from November to May. Within the region there is relatively little spatial variation in either the timing of fire starts or proportion of area burned per month, although the total area burned is invariably greater on the east side of the Cascades than the west (Westerling et al. 2003). In the wettest forests of the study region, the fire season is delayed by several weeks. For example, observed and simulated wildfire data for the Olympic Mountains, Washington, suggest few or no large fires occur in June, greater than 40% occur in July, greater than 40% occur in August, and slightly more than 10% occur in September (Agee and Flewelling 1983). Results from coastal Oregon are similar (Agee and Krusemark 2001). (3) Any variability in the timing of fires within the fire season that does occur would most likely weaken the observed associations between BAI and climate. Consequently, any associations that we do identify are more likely to underestimate the magnitude of the actual relationship than to overstate it. (4) The relationships that we identify here can be directly compared to observations made for individual large fires (e.g., Countryman et al. 1969, Sando and Haines 1972, Finklin 1973, Street and Alexander 1980) and quantitative analyses of shorter records (e.g., Street and Birch 1986, Westerling et al. 2003) to assess consistency.

## METHODS

We considered several possible methods of subdividing the study area into regions of coherent fire patterns, including cluster analysis, classifications based on vegetation, climate, and fire regime, and eigenvector techniques. We chose to use empirical orthogonal function (EOF) analysis because it incorporates most of the advantages of the other techniques considered, but has several key advantages. In particular, EOF analysis is able to identify patterns in area burned that might overlap in space (see Schroeder [1969]). EOF analysis is a type of eigenanalysis that identifies structures that explain the maximum amount of variance in a two-dimensional data set. In this application the structure dimension consists of 20 National Forests, and the sampling dimension is time, with 48 yr. Eigenanalysis of this matrix produces a set of spatial structures in the first dimension (EOFs) and corresponding structures in the sampling dimension (principal components [PCs]). Each PC describes the variability of the associated EOF over time. Each EOF is orthogonal to all other EOFs, and each PC is similarly orthogonal to all other PCs. Each EOF/PC pair has a corresponding eigenvalue that describes the variance explained by the pair.

The atmospheric circulation anomalies associated with each EOF were determined by regressing the 500-hPa anomaly field onto the associated PC time series. Suppose  $\mathbf{P}$  is a vector of the PC time series with  $n$  observations, and  $\mathbf{H}$  is an  $n \times m$  matrix of 500-hPa height anomalies for a given month of the fire season, where  $m$  indicates the number of gridpoints for which 500-hPa height anomalies were considered. The vector  $\mathbf{K}$  can be calculated as

$$\mathbf{K} = n^{-1}\mathbf{P}\mathbf{H}. \quad (1)$$

$\mathbf{K}$  will be of length  $m$  and can be mapped to show the anomaly field associated with a 1-SD perturbation in  $\mathbf{P}$ . These maps are commonly called spatial regressions, or map projections, because a time-varying spatial field is being regressed (or projected) onto a time-varying vector. Maps of  $\mathbf{K}$  were developed for each month of the fire season (May–September). The correlation between 500-hPa height at each gridpoint in  $\mathbf{K}$  and the relevant BAI was also calculated, and regions where the association is significant ( $\alpha < 0.05$ ) are shown on the figures as dark shaded regions. Although some spurious results are expected, the strong spatial autocorrelation in the atmosphere means that most of the regions identified in this analysis represent important “centers of action,” which are contributing to the increase in area burned downstream. The variance in  $\mathbf{P}$  that can be explained by  $\mathbf{K}$  can be estimated by calculating  $k$ , the expansion coefficient time series of  $\mathbf{K}$ ,

$$k = \mathbf{H}\mathbf{K} \quad (2)$$

which provides a vector describing the variability in  $\mathbf{K}$  over time. The correlation between  $k$  and  $\mathbf{P}$  provides

an estimate of the variation in  $\mathbf{P}$  that can be linearly explained by  $k$ , but should be interpreted cautiously as  $\mathbf{K}$  was initially defined using  $\mathbf{P}$ .

This analytical approach assumes that there is a linear association between atmospheric variability and wildfire activity. It is possible however that extreme wildfire years may occur under a much narrower set of climatic conditions than less extreme years. In this scenario the linear association could appear quite weak, and the underlying forcing pattern might be missed altogether. In order to assess this scenario we used superposed epoch analysis (SEA) to characterize the 500-hPa height anomalies during the smallest- and largest-fire years. The five years with the largest area burned and the five years with the smallest area burned were identified. The mean and standard deviation in the 500-hPa height field for the large- and small-wildfire years were calculated. A two-sample  $t$  test was used to identify regions where 500-hPa height anomalies are significantly different between the epochs. For display purposes, the small-fire-years composite was subtracted from the large-fire-years composite to emphasize the difference in circulation between the two epochs. Additionally, these map composites were compared to the spatial regression maps for consistency and magnitude.

The role of antecedent climate conditions in preconditioning forests for large wildfire years was explored using cross-correlation analysis. The correlation between the regional BAI (and PCs), and total precipitation, mean temperature, and PDSI was calculated for each month of the fire season (May–September) as well as the 12 preceding months. These results provide some insight into the relative roles of seasonal-scale climatic variability and shorter-term (presumably synoptic-scale) processes in driving large-wildfire years. Similar to the analysis of 500-hPa described above this cross-correlation assumes a linear association between area burned and antecedent climate. For comparative purposes we also calculated composite maps showing the mean PDSI for the most extreme wildfire years.

## RESULTS AND DISCUSSION

### *Composite burned area index*

Projecting the 500 hPa height field onto the region-wide composite BAI reveals a significant association between increases in area burned and increases in 500-hPa height over western North America during the height of the fire season: June, July, and August (Fig. 2). This pattern is consistent with the development of a high-pressure blocking ridge upstream from the study area, which would divert storm tracks out of the region and reduce relative humidity. These events can also cause extremely warm and dry easterly winds that dramatically increase the fire hazard. Additionally, there is a significant correlation with lowered 500-hPa heights in the central and northern Pacific Ocean in

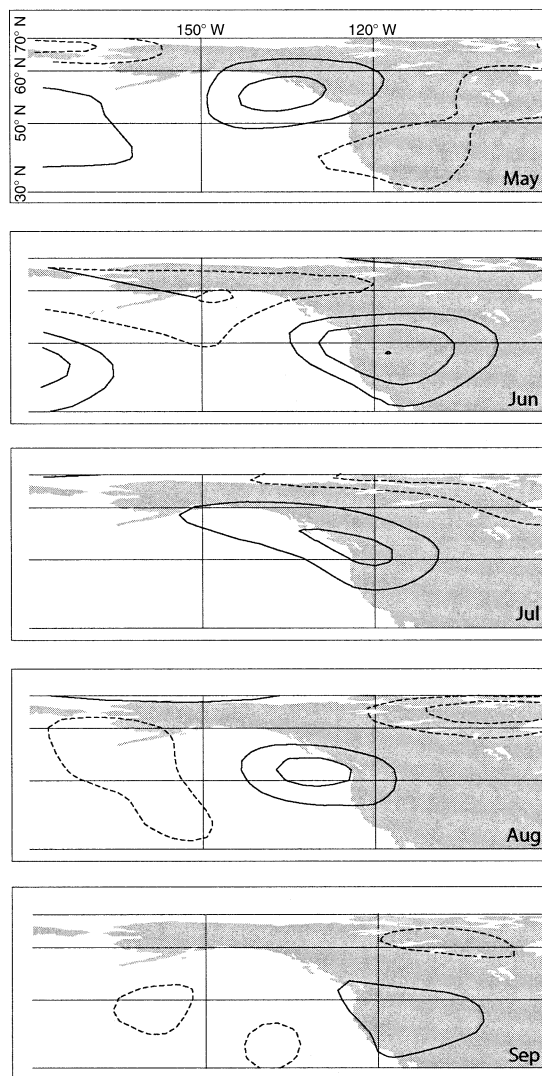


FIG. 2. The 500-hPa height anomaly field projected onto the regional burned area index (BAI), May–September. This pattern describes the atmospheric variability associated with a one-standard-deviation perturbation in BAI. The contour interval is 5 m, with positive anomalies indicated by a solid contour, negative anomalies by a dashed contour, and the zero line not shown. Cross-hatched regions indicate that the correlation at that gridpoint is significant at the 95% confidence level.

August, which would enhance the east-to-west pressure gradient.

The correlation between the expansion coefficient time series of the projected patterns and the regional BAI ranges from 0.35 to 0.51 over the fire season (Fig. 3, triangles). This correlation improves substantially when either the maximum or mean fire-season value of the expansion coefficient time series is considered ( $r = 0.58$  and  $0.65$ , respectively). This finding is consistent with the hypothesis that several weeks of fire-conducive weather at any point in the fire season can lead to increases in area burned, but that the timing of

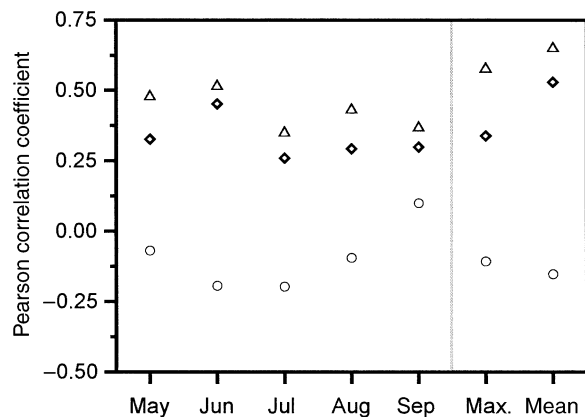


FIG. 3. The correlation between the expansion coefficient time series of the 500-hPa map pattern associated with all years (triangles), the five largest-fire years (diamonds), the five smallest-fire years (circles), and the composite burned area index (BAI). The correlation was calculated for all months of the fire season (to the left of the vertical gray line) as well as the maximum (Max.) and mean fire-season indices (to the right of the vertical gray line).

fire weather is less important than the magnitude (i.e., maximum blocking index) or persistence (i.e., mean blocking index).

The magnitude of the 500-hPa height anomalies shown in Fig. 2 is relatively modest: only  $\sim 15$  m ( $\sim 0.5$  SD). This result implies either that area burned is very sensitive to 500-hPa height anomalies or that there is a lot of noise in the model. Some insight into the relationship can be gained by considering the results of the SEA (Fig. 4). Composite maps of the five smallest-fire and five largest-fire years indicate a strong association between increased (decreased) 500-hPa height and increased (decreased) area burned. The magnitude of these 500-hPa height anomalies is substantially larger than seen in the map projections, up to  $+45$  m, although the structure of the patterns is very similar. These results suggest that especially small- and large-fire years are more sensitive to atmospheric variability than are moderate-fire years. Indeed, projecting the 500-hPa height field onto the BAI for the remaining years (not the five smallest- or largest-fire years) reveals virtually no association between atmospheric variability and fire extent (results not shown). Interpreted together these results suggest that extreme fire years (both large and small) are more sensitive than moderate-fire years to variability in the mid-tropospheric height surface.

By deriving the expansion coefficient time series of the large- and small-fire-year composite maps it is possible to calculate the correlation between the patterns identified in the SEA and area burned. Unlike the analysis described above these time series are largely independent of the BAI data and probably provide a more robust estimate of the strength of the linear association between atmospheric circulation and wildfire activity.

The correlation between the index based on the large-fire-years composite and area burned is significant and suggests at least a moderate linear association between the blocking structure and wildfire activity (diamonds in Fig. 3). In contrast, the correlation between the index based on small-fire years and area burned is very weak (circles in Fig. 3) and provides little support for a linear relationship.

Scatterplots of these circulation indices vs. BAI provide some insight into the nature of the association between blocking (anti-blocking) activity and large- (small-) wildfire years (Fig. 5). The large-fire-year composite index suggests that the atmosphere imposes a strong constraint on fire activity. Eight of the 10

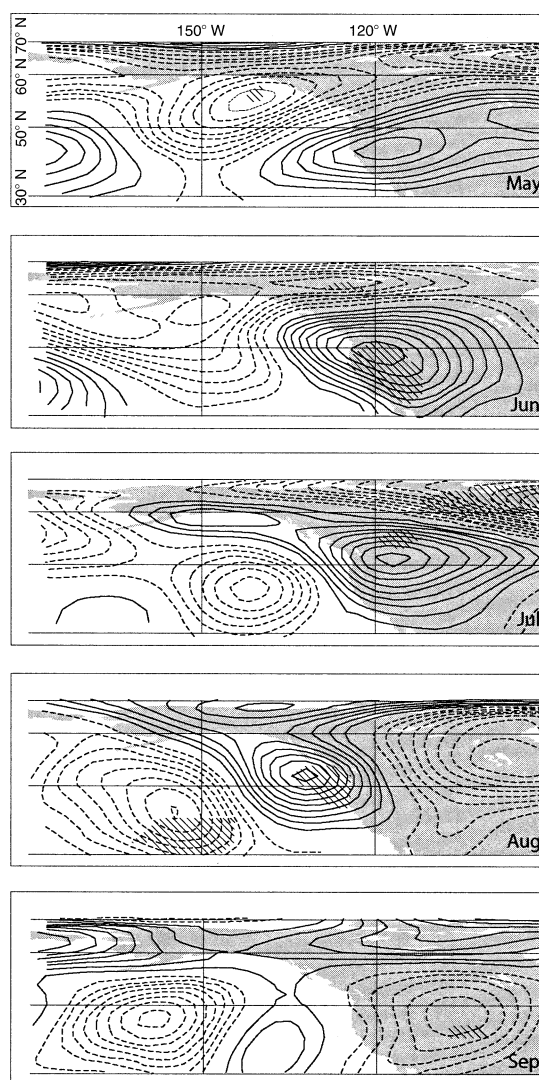


FIG. 4. Difference in the 500-hPa height field between the five largest- and smallest-fire years in the regional burned area index (BAI) from May to September. Contour intervals are as in Fig. 2. Regions where the difference between large-fire and small-fire years is significant at 95% confidence (two-sample  $t$  test used) are indicated by hatching.

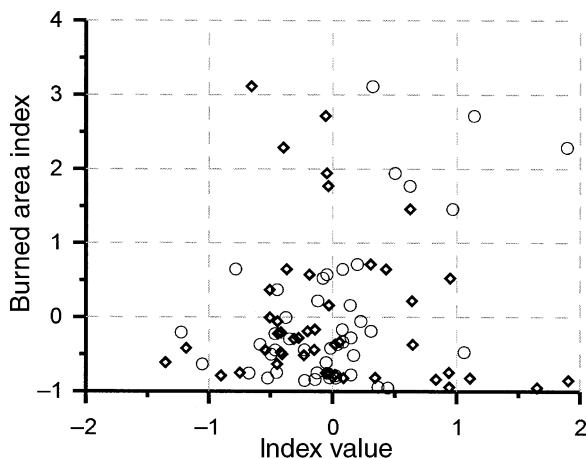


FIG. 5. Scatterplots of the regional burned area index (BAI) vs. the mean annual large-fire composite index (circles) and small-fire composite index (diamonds).

largest-fire years occur during summers with positive mean blocking index values. Only 1977 stands out as a year with a high blocking index value but little wildfire activity. In contrast to this control on large-wildfire years, only five out of the 10 smallest-wildfire years occur under negative mean blocking index conditions. The scatterplot of the small-fire composite index vs. BAI presents a less obvious picture. While eight of the 10 smallest-fire years occur under a positive index, a number of very-small-fire years also occur under a strongly negative index. There are several possible explanations for this scenario: (1) the conditions that contribute to very-small-fire years may be more spatially heterogeneous than was observed for large-fire years. That is, a wide range of conditions may lead to small area burned in any given year. This interpretation is consistent with the observation that the larger-fire years exhibit an inverse association to this index whereas the smaller years exhibit much greater scatter. (2) The time scale associated with the conditions that lead to particularly small-wildfire years may be shorter than a month and therefore are not evident in the monthly climatic variables considered in this analysis. For example, even a few days of heavy rain could suppress any active wildfires and reduce the probability of new ignitions even in the event of weather conditions that would otherwise be highly favorable for wildfire activity. (3) The fire data themselves may be spatially heterogeneous. That is, there may be a narrow range of conditions that lead to region-wide reductions in area burned, but a more diverse set of conditions that lead to more localized reductions. This last possibility is explored in greater detail in the next section.

In order to assess the role of antecedent climate in preconditioning forests to burn we calculated lagged correlations between BAI and monthly PDSI, temperature, and precipitation for the interval starting one year prior to the fire season. The correlation between

BAI and PDSI exhibits a region-wide coherence, with increases in area burned associated with increased drought throughout spring and summer of the current year (Fig. 6). The association with PDSI in the winter preceding the fire year is weak and does not exhibit spatial coherence, suggesting that winter climatic variability does not exert an important control on wildfire activity.

The correlations with precipitation and temperature exhibit patterns consistent with the results for PDSI (not shown). Increases in area burned are associated with increased temperature in March through August. There is a weak association with cooler than average temperatures in the preceding autumn and to above average temperatures in the preceding summer. The association with precipitation is more highly variable, with strong correlations exhibited only at the height of the fire season; increases in fire are associated with reduced precipitation in June through August of the fire season. Prior to April of the fire year the correlations to precipitation are generally weak, exhibit both positive and negative signs, and show no obvious pattern. Interpreted together, these results suggest that the combination of temperature and precipitation is more important in preconditioning forests to burn than either of them individually.

In order to estimate the strength of the association between regional drought and area burned we calculated the mean monthly PDSI value for all climate divisions in Washington and Oregon. The correlation between this regional PDSI record and area burned is  $-0.31$ ,  $-0.30$ , and  $-0.37$  for the months of June through August, respectively. The magnitude of this correlation decreases rapidly both before and after the fire season, with nonsignificant correlations exhibited in April before the fire season ( $r = -0.25$ ) and in October following the fire season ( $r = -0.25$ ).

The results presented here suggest that climatic variability is an important cause of variation in area burned by wildfire in the American Northwest. Blocking ridges, evident in the 500-hPa height field, contribute to increased drought stress in spring and summer of the fire year. These soil moisture deficits contribute to reduced fuel moisture, increasing the flammability of the landscape. The associations observed in this analysis were limited primarily to spring and summer months, implying that variability in winter conditions contributes little to wildfire activity in the following summer. This finding has important implications for the forecasting of seasonal wildfire severity, as wintertime climatic variability is much better understood than summertime variability (Kumar and Hoerling 1998). Similarly, El Niño/Southern Oscillation (ENSO) and Pacific Decadal Oscillation (PDO) express themselves most strongly in winter months in the Pacific Northwest (Ropelewski and Halpert 1986, Yarnal and Diaz 1986, Mantua et al. 1997, Zhang et al. 1997, Gershunov and Barnett 1998), implying that skillful ENSO or PDO

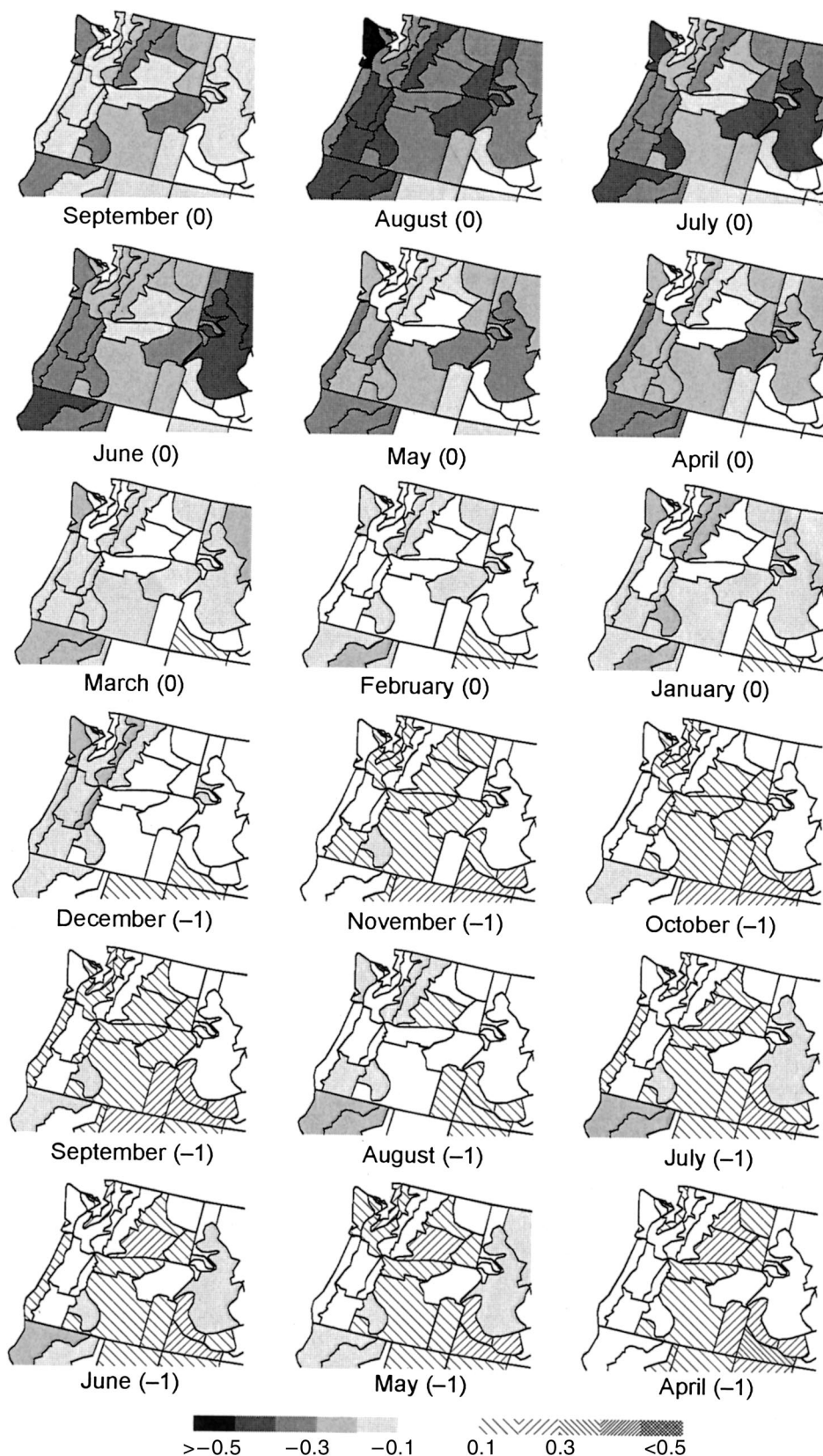


FIG. 6. Lagged correlation between the regional burned area index (BAI) and Palmer drought severity index (PDSI). Inverse correlations are shown in solid shades and indicate a correspondence between increases in area burned and enhanced drought conditions. Numbers in parentheses following months indicate the year: 0, current year; -1, one year before.

forecasts would contribute little information to a fire-season forecast.

ENSO is a pattern of ocean-atmosphere variability that is characterized by episodic warming (cooling) in the western tropical Pacific and weakened (strengthened) trade winds. The North Pacific Ocean typically exhibits an enhanced (weakened) wintertime Pacific North America (PNA) pattern in response to warm (cool) ENSO events (Yarnal and Diaz 1986). Associated teleconnections cause the Pacific Northwest normally to be warm and dry (cool and wet) during winter months (Ropelewski and Halpert 1986, Yarnal and Diaz 1986). The return interval for strong ENSO events is typically 3–7 yr. The PDO is an ENSO-like pattern of variability, with similar teleconnections, but is most strongly expressed in the extra-tropical North Pacific (Mantua et al. 1997). It is characterized by variability at interannual to interdecadal scales, but also appears to shift abruptly between warm and cool mean states every few decades (Mantua et al. 1997, Gedalof and Smith 2001). Warm conditions persisted from approximately 1925 to 1946 and from 1977 to approximately 1989, and cool conditions persisted prior to approximately 1925 and from 1947 to 1976 (Mantua et al. 1997, Hare and Mantua 2000).

In order to test the hypothesis that these patterns are not important forcing mechanisms for extreme wildfire years we compared BAI during warm (i.e., El Niño) and cool (La Niña) ENSO years and in the warm and cool phases of the PDO using a two-sample *t* test. These tests confirmed that there is no significant difference in area burned between warm and cool ENSO events ( $P = 0.255$ ) and between warm and cool PDO regimes ( $P = 0.178$ ). As an additional measure we calculated the correlation between the Cold Tongue Index (CTI), an index of ENSO activity (Zhang et al. 1997), the PDO index (Mantua et al. 1997), and the regional BAI. This analysis supported the finding that there is no association with ENSO activity ( $r = -0.01$ ,  $P = 0.953$ ), but suggests that there is at least a modest association between the PDO and area burned ( $r = 0.40$ ,  $P = 0.005$ ). This latter disparity can be explained by the fact that interannual variability in the PDO often exceeds the inter-regime variability (Fig. 7). Although only six out of the 10 largest-fire years occurred during the warm phase of the PDO, seven of the 10 largest years followed winters when the PDO index was positive, and eight of the 10 smallest-fire years occurred following winters when the PDO index was negative. Wildfire extent is therefore more closely related to this higher-frequency variability than to decadal variability. However, this finding does imply that in the long run there will be increases in area burned during the warm phase of the PDO, because the PDO index will be on average higher during these regimes. It is likely that the short time series considered in this analysis (slightly less than one complete cycle of the PDO) does not provide a sufficiently large sample to detect this dif-

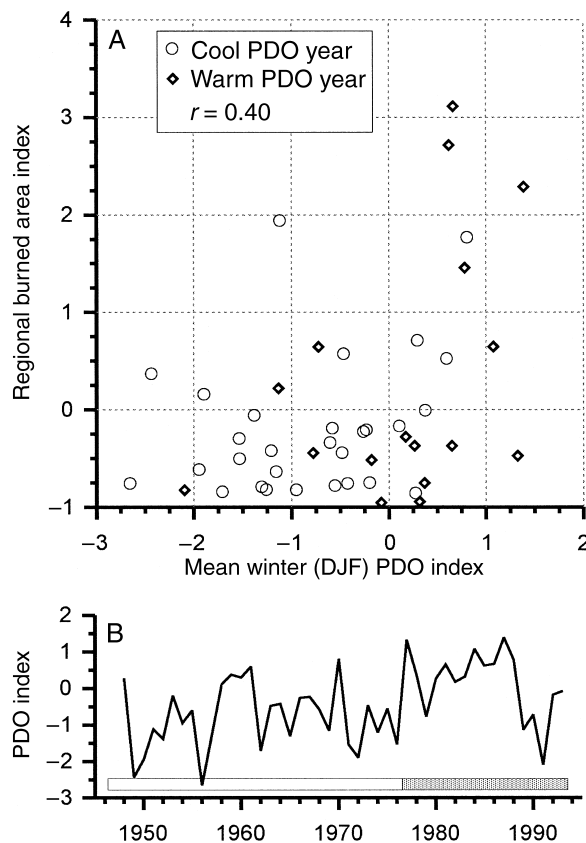


FIG. 7. (A) Scatterplot of the regional burned area index (BAI) vs. the mean winter (December, January, February) Pacific Decadal Oscillation (PDO) index. Warm PDO regime years (1978–1994) are indicated by diamonds, and cool years (1949–1976) are indicated by circles. (B) The time evolution of the PDO index, showing the transition from cool to warm conditions between 1976 and 1977.

ference. Alternatively, there may be a signal related to fire management practices that is obscuring the underlying nature of the relationship.

#### Regionalized burned area indices

The leading four eigenvectors were retained from the EOF solution, collectively explaining 54% of the variance in area burned in the 20 National Forests. The eigenvalues associated with these patterns were all significantly greater than 1.0 (North et al. 1982), and Monte Carlo simulations suggested that the resulting patterns were robust to the choice of years included in the analysis (results not shown). The eigenvectors respectively explain 25, 15, 10, and 9% of the total variance in annual area burned. The leading mode of variability (EOF1) is characterized by increases in area burned throughout most of the region, although the National Forests in northwestern Washington and central Oregon load weakly on this EOF (Fig. 8A). The National Forests that load strongly on EOF1 comprise a wide range of forest types; however, none of the more mesic forest types load strongly on this EOF.

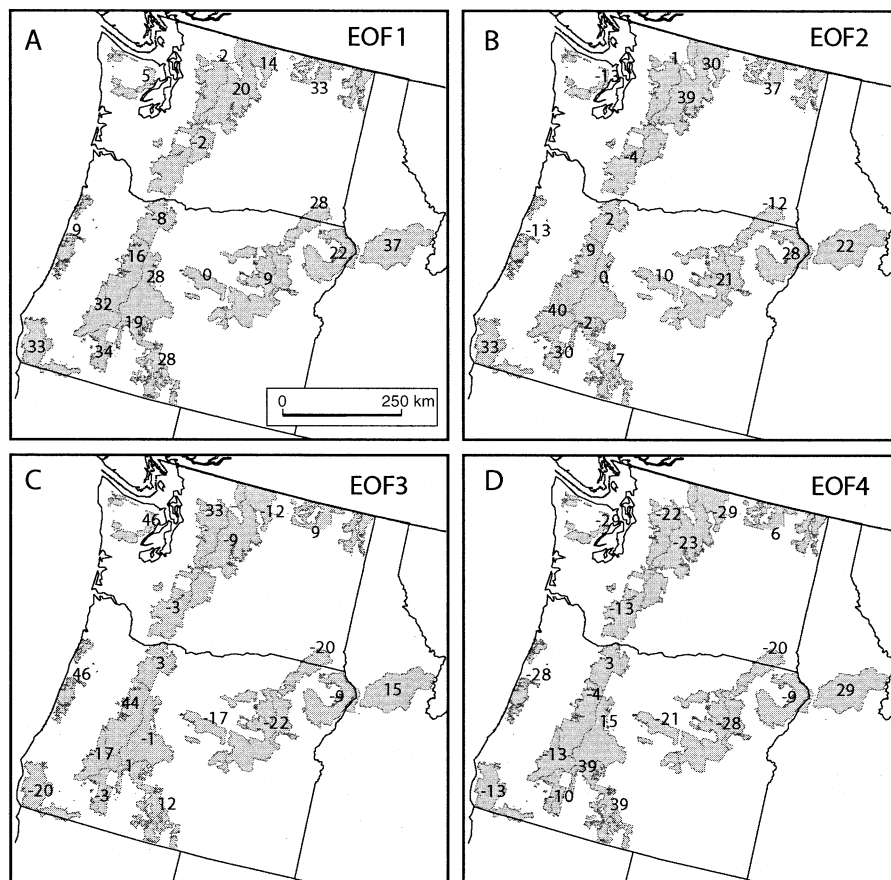


FIG. 8. Loading values ( $\times 100$ ) for the leading four empirical orthogonal functions (EOFs) of area burned. EOFs 1–4 explain 17%, 13%, 12%, and 10% of the variance in burned area index (BAI), respectively.

Projecting the 500-hPa height field onto PC1 reveals a significant association between this pattern in burning and positive height anomalies over western North America (Fig. 9). This feature appears to migrate southwestward over the course of the fire season, starting out in central Canada in May and ending up over the central North Pacific in September. While the feature is absent in July the mean circulation conditions in this month do not normally inhibit fire ignition or spread. One possible interpretation of this result is that the differences between small- and large-fire years are a consequence of burning that occurs outside of the usual fire-season maximum. That is, because mid-summer climatological conditions are naturally conducive to wildfire activity, variability in area burned is most sensitive to conditions in the early or late fire season. A corollary to this hypothesis is that the total length of the fire season is more important than the magnitude of blocking highs or the intensity of drought at the apex of the fire season. Although the apparent migration of this blocking feature is consistent with the "Great Basin High" pattern described by Schroeder (1969), the time evolution seen here is clearly much longer than he intended.

Map composites of 500-hPa height anomalies for the five smallest- and largest-fire years captured by PC1 are consistent with the relationships seen in the spatial regressions (Fig. 10). The five largest-fire years are characterized by pronounced positive height anomalies over western North America in May, June, July, and August and, except for July, negative height anomalies over the central Pacific. In spite of the few degrees of freedom in this analysis the difference between small-fire and large-fire years is statistically significant in May, June, and July ( $P < 0.05$ ). The map projection for September reveals a significant association to elevated 500-hPa heights over the central Pacific and reduced heights over western North America. These patterns are nearly identical to those identified in the analysis of the regional BAI (see Fig. 2), but in every month considered the magnitude of the 500-hPa height anomalies observed is greater for PC1 than for the regional BAI. This finding implies that the EOF analysis is effectively capturing the coherent signal in the area burned record and that atmospheric forcing is responsible for at least some of the coherence in this signal. This result could be due to the efficiency of eigenvector techniques at extracting meaningful patterns from

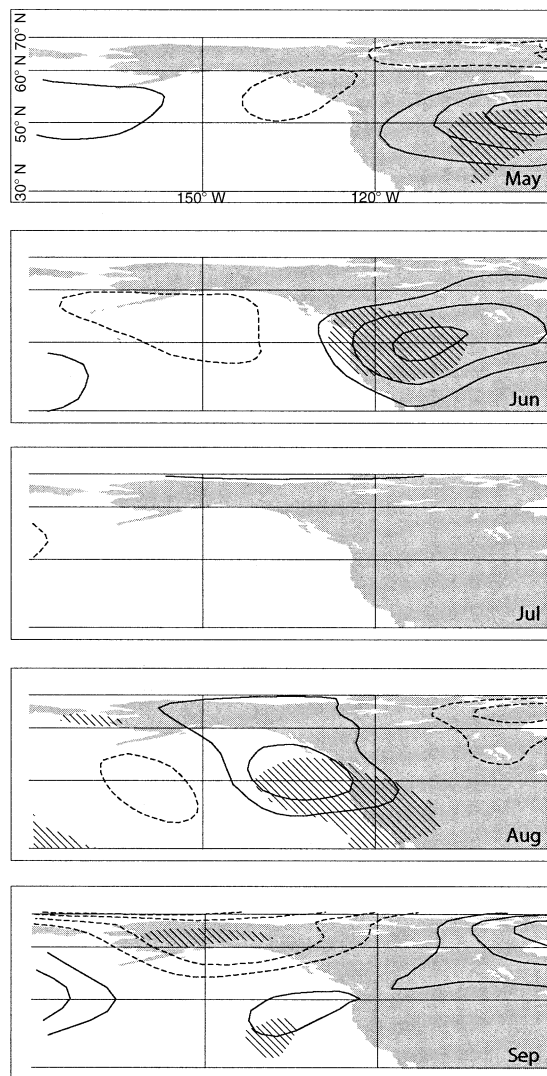


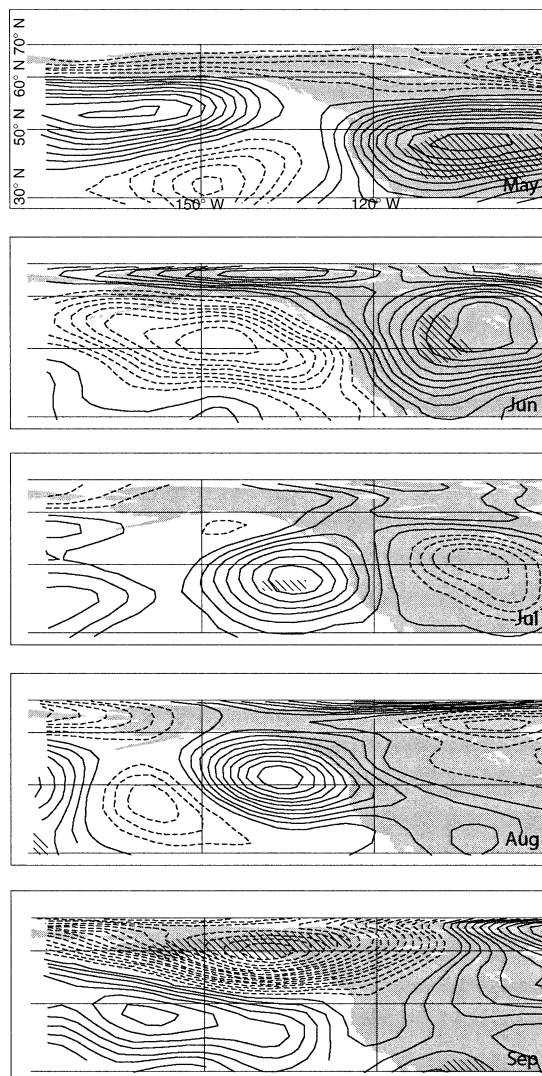
FIG. 9. The 500-hPa height anomaly field projected onto principal-components axis 1, PC1 (contours and significance are as shown in Fig. 2).

noisy data (Gauch 1980), or it could be that the regional BAI is in fact composed of multiple signals, only one of which is forced by this pattern of atmospheric variability.

Lagged correlations between PC1 and PDSI suggest that increases in area burned are associated with enhanced regionwide drought in the winter, spring, and summer leading up to the fire season (Fig. 11). Consistent with the results from the 500-hPa height field the magnitude of the correlation coefficients is greater for the EOF results than for the regional BAI. For comparison, the correlation between PC1 and the mean Washington and Oregon PDSI is  $-0.59$ ,  $-0.55$  and  $-0.61$  for June, July, and August, respectively, of the fire season. This correlation remains significant at increasing lags, back to October of the preceding year. Together these results suggest that this pattern of wild-

fire variability is associated with drought conditions that initiate in the preceding winter and persist through the wildfire season, accompanied by summertime blocking events.

The second EOF of area burned is characterized by a northeast–southwest dipole (Fig. 8B), with increases in area burned at Colville, Okanogan, Wenatchee, and (to a lesser extent) Nez Perce and Wallowa-Whitman National Forests, corresponding to reductions at Siskiyou, Umpqua, and Rogue River National Forests. There are some important differences between the two regions in terms of their ecology: Colville, Okanogan, and Wenatchee contain extensive stands of pure Douglas-fir. Siskiyou, Umpqua, and Rogue River represent



Small fire years: 1971, 1974, 1975, 1957, 1978  
Large fire years: 1987, 1988, 1994, 1992, 1959

FIG. 10. Difference in the 500-hPa height field between the five largest- and smallest-fire years represented by principal-components axis 1, PC1. Contours and statistical significance are shown as in Fig. 4.

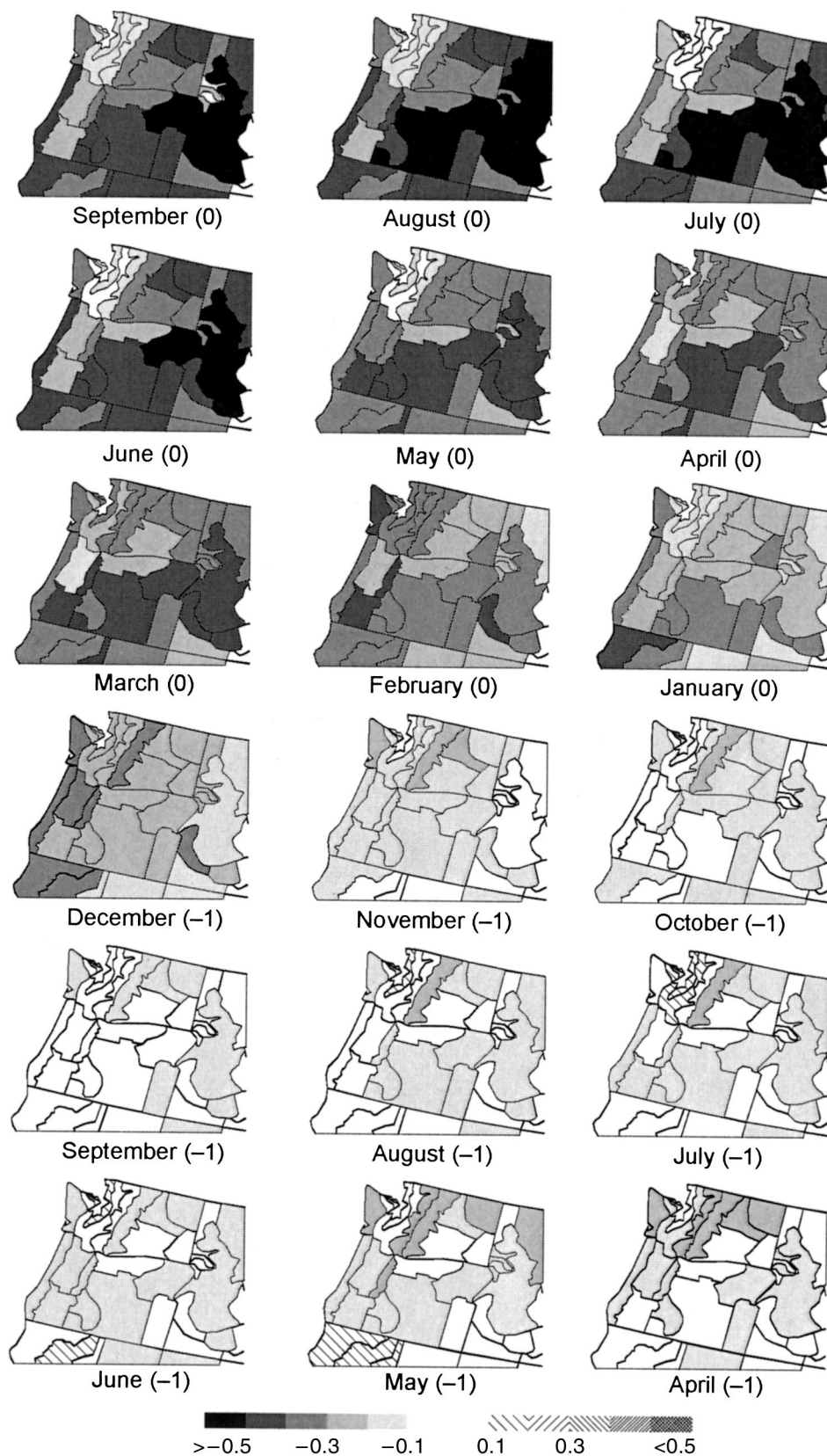


FIG. 11. Lagged correlation between principal-components axis 1 (PC1) and the Palmer drought severity index (PDSI). Inverse correlations are shown in solid shades and indicate a correspondence between drought and increases in area burned. Numbers in parentheses following months indicate the year: 0, current year; -1, one year before.

a transitional zone between the temperate forests of the Pacific Northwest and the drier, more Mediterranean forests of the Pacific Southwest. These latter forests also contain a large portion of red fir that is distinct within the study region. However, these two centers of action also exhibit many similarities to other forests of the region that do not load particularly strongly on this EOF. This observation, along with the strong spatial arrangement of the EOF loadings, suggests that the pattern is driven largely by top-down (i.e., atmospheric/climatic) rather than bottom-up (i.e., ecological) controls.

Projecting the 500-hPa height field onto PC2 reveals generally weak associations with atmospheric circulation. The only significant association that seems relevant occurs during July and is characterized by increased 500-hPa heights over western North America and decreased heights over the Gulf of Alaska (Fig. 12). This pattern resembles the summertime Pacific North America (PNA) pattern (Knox and Lawford 1990) and is virtually identical to patterns associated with severe wildfire years in western Canada (Johnson and Wowchuk 1993, Skinner et al. 1999). This PNA-like structure is also present in the map composites of the five largest-fire years (results not shown). These results cannot be directly compared to the regional BAI map composites because large positive values indicate increases in area burned in the northeastern portion of the region but reductions in area burned in the southwest. Therefore the five smallest values do not indicate small-fire years, but rather years when there were increases in area burned in the southwest and reductions in the northeast. Nonetheless, the composite maps do indicate the presence of reduced 500-hPa heights over the North Pacific/Gulf of Alaska during high PC2 index years in the months of May, June, and July. The PNA pattern has been shown in winter months to divert precipitation away from the Pacific Northwest northwards into British Columbia and Alaska, with a second storm track often directed into the southwestern United States (Trenberth and Hurrell 1994). In summer months this pattern might deliver precipitation to southern Oregon, reducing the fire hazard there, while diverting precipitation away from northern Washington and thereby increasing the fire hazard there.

Lagged correlations between PC2 and PDSI reveal very weak correspondence between area burned and antecedent drought conditions (results not shown). The correlation to mean Washington and Oregon PDSI is not significantly different from zero at any point of the fire season or the preceding months ( $r = -0.06$ ,  $-0.09$ , and  $-0.11$  for June, July, and August, respectively). These findings suggest that a summer PNA pattern can contribute to a northeast–southwest dipole in area burned. This pattern may be weakly modulated by local drought, but is not controlled to any significant extent by regional drought severity. This pattern appears to be related to the arrangement of the National Forests

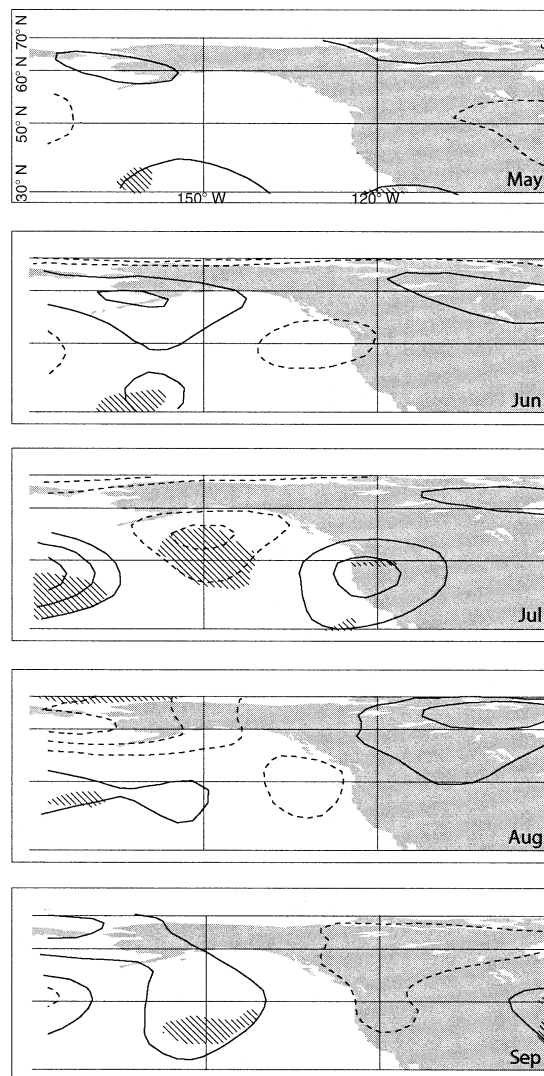


FIG. 12. The 500-hPa height anomaly field projected onto principal-components axis 2, PC2 (contours and significance are shown as in Fig. 2).

in space rather than their underlying ecology or fire regime. The EOF/PC pair that was identified in this analysis is clearly not a simple linear pattern and may not be well defined by the analysis.

EOF3 is characterized by increases in area burned in Olympic, Mount Baker-Snoqualmie, Siuslaw, and Willamette National Forests and reductions at Siskiyou, Umpqua, Ochoco, Malheur, and Umatilla National Forests (Fig. 8C). This pattern is consistent with increased fire activity at the wettest forests of the region, in particular at the two National Forests with temperate rain-forest components, but also at Mount Baker-Snoqualmie and Willamette, which have extensive western hemlock and Pacific silver fir components. Although Siskiyou National Forest also contains these mesic forest types they are generally restricted to a narrow coastal band that is defined by the landward extent of fog

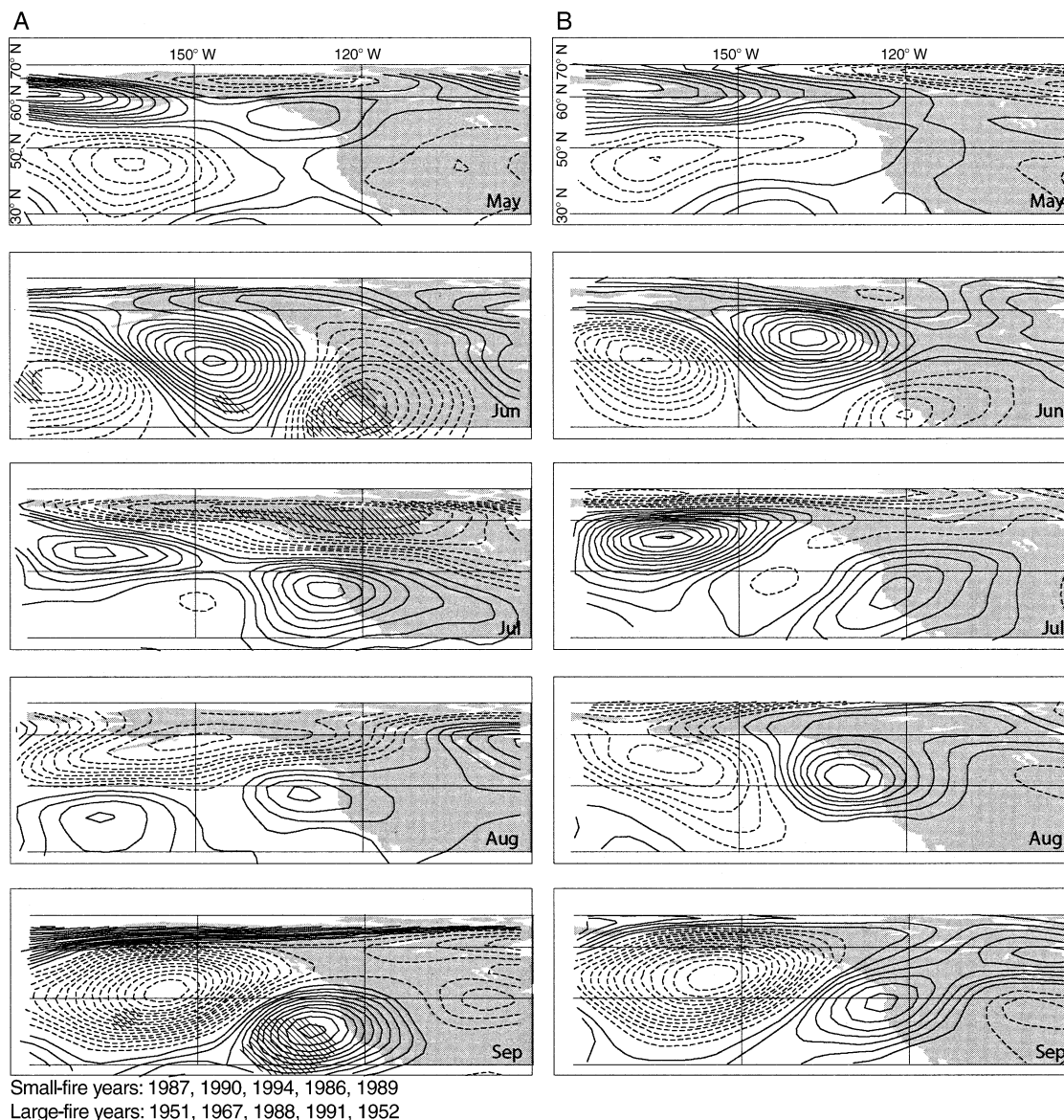


FIG. 13. (A) Difference in the 500-hPa height field between the five maximum and the five minimum values of principal-components axis 3, PC3 (contours and significance are shown as in Fig. 4). (B) Composite map of the three large-fire years (1951, 1967, and 1988) represented by PC3 (contours are shown as in Fig. 2).

occurrence. Beyond this fog belt the forests are characterized by much drier vegetation types than occur at more northern coastal forests (Franklin and Dyrness 1973), and historical fire occurrence is generally more frequent and less severe (Agee 1991).

Projecting the 500-hPa height anomaly field onto PC3 reveals virtually no linear correspondence between atmospheric circulation and annual area burned (results not shown). In contrast, however, the map composites indicate an association between persistent blocking features over western North America and the five most extreme fire years represented by PC3 (Fig. 13A). This relationship is more readily apparent if the (only) three

very large events contained in the record are considered (Fig. 13B). This 500 hPa height surface is similar to the blocking structures identified for the regional analysis (see Fig. 4) and for PC1 (see Fig. 9); however, the system appears to be located further west throughout most of the fire season. This pattern would be especially conducive to anomalous easterly winds in the coastal region, as air circulates clockwise around the high.

Lagged correlations to the PDSI reveal a weak association between area burned and drought in western Washington during the fire season. This result seems counterintuitive, because these forests are typically too moist to carry fire in most years. One possible expla-

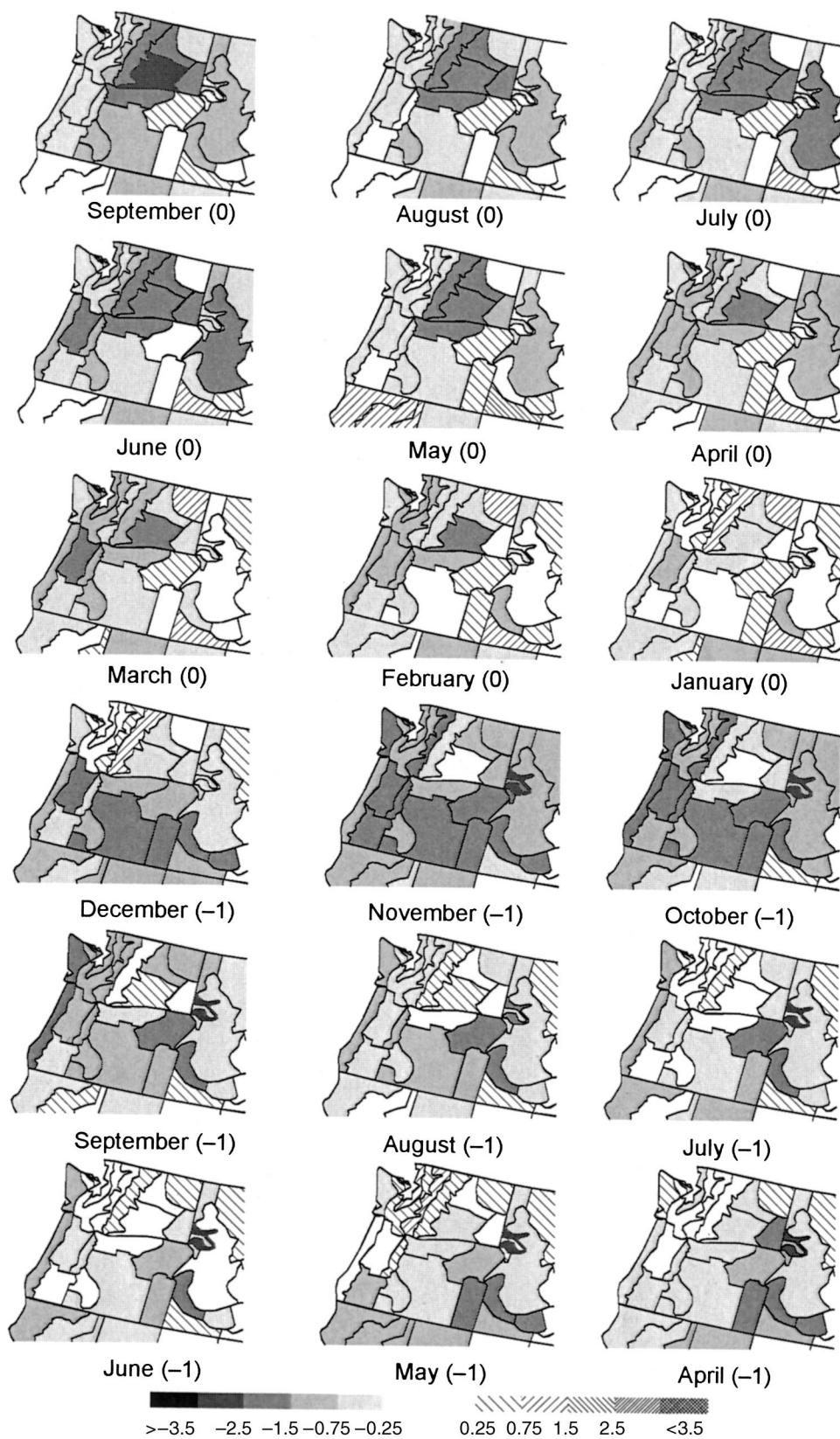


FIG. 14. Composite Palmer drought severity index (PDSI) values for the three largest-fire years (1951, 1967, and 1988) represented by principal-components axis 3, PC3.

nation for this result is that these forests are strongly ignition limited. That is, drought conditions alone may not lead to increases in area burned unless there is also a source of ignition. Additionally, because there have been very few large-fire years in Olympic and Siuslaw National Forests (and therefore in PC3) linear analyses will almost certainly fail to identify the causes of these extreme fire years. In order to investigate this possibility we developed composite maps of the three large-fire years represented by PC3 (Fig. 14). This analysis reveals good correspondence between drought west of the Cascade Mountains and large area burned for the interval beginning in the preceding fall and continuing through the fire season.

These results imply that in Northwestern coastal forests large-fire years occur only when drought persists through several seasons leading up to the fire season, followed by summertime circulation anomalies that favor hot, dry, easterly winds. This pattern is consistent with the ecology of these forests, which tend to be characterized by complex age structures and abundant woody debris, but a microclimate that favors high relative humidity and rapid decomposition of organic material (Chen et al. 1999). This environment contains substantial potential fuel, but requires exceptional circumstances to dry out the landscape sufficiently that it will burn readily (Agee 1993). This hypothesis is consistent with the observed seasonality of large fires, which is restricted to the later portion of the fire season (Agee and Flewelling 1983). These forests may also be ignition limited; even when fuels are dry, increases in area burned by wildfire may not necessarily follow.

EOF4 is characterized by increases in area burned at a few National Forests in southern Oregon (Fremont, Winema, and Deschutes) as well as at Nez Perce National Forest and reductions at most other forests. These forests are among the driest of the region and are all characterized by extensive stands of lodgepole and ponderosa pine. Summertime precipitation often totals <2 cm, and temperatures are the highest of the study area (Jackson and Kimerling 1993). The 500-hPa height field associated with this pattern in burning is significantly lower than normal over western North America in June, July, and September, although the magnitude of these departures is generally quite small (results not shown).

The SEA again shows a stronger and more consistent relationship (Fig. 15) than the map regression. Large values of PC4 occur when very low 500-hPa heights persist over the study region throughout the fire season. At these particularly dry forests this circulation pattern would bring summer cyclones with lightning and strong winds, but very little precipitation, thereby providing a source of ignition and a cause for rapid wildfire spread. In contrast, these same storms could deliver significant rainfall to regions west of the Cascade Mountains and to more northerly interior regions, thereby reducing the fire hazard at those forests. The

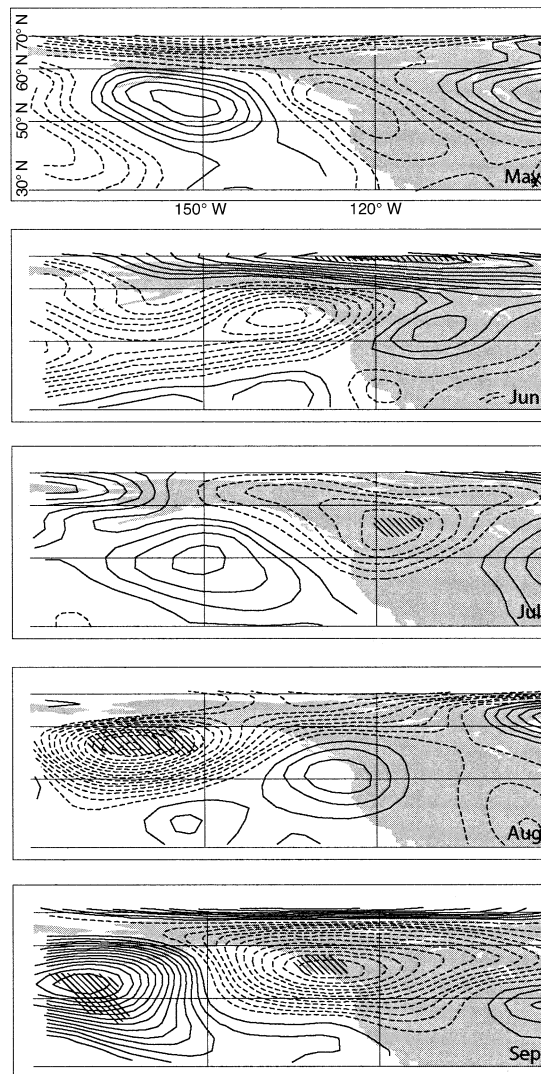


FIG. 15. Difference in the 500-hPa height field between the five maximum and the five minimum values of principal-components axis 4, PC4 (contours and significance are shown as in Fig. 4).

five minimum values of PC4 are associated with approximately opposite conditions, that is, anomalous high pressure over western North America. This pattern is comparable to the blocking ridges described above and would lead to increases in area burned (at those forests that load negatively on EOF4) for the reasons already discussed. Most of the forests that load strongly negatively on EOF4 load weakly on EOF1, the other pattern in burning that shows a good relationship to persistent blocking features. These results imply that most of the forests of the region do show increases in area burned in response to blocking events, but that there are differences in either the atmospheric forcing or the ecological response to these events.

Some insight into the cause for these differences can be gained by examining the lagged correlation to PDSI:

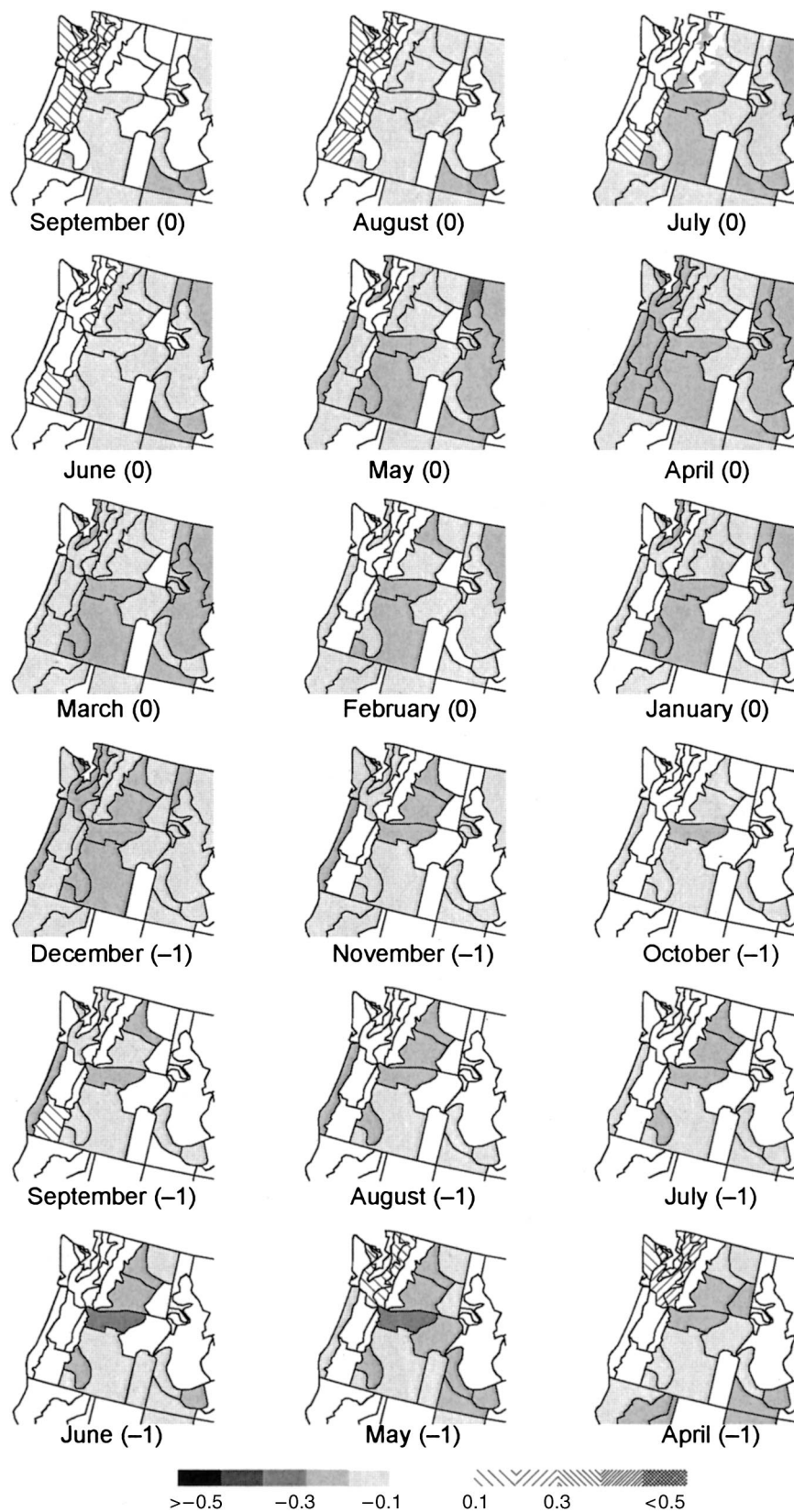


FIG. 16. Lagged correlation between principal-components axis 4 (PC4) and the Palmer drought severity index (PDSI). Inverse correlations are shown in solid shades and indicate a correspondence between drought and increases in area burned.

TABLE 2. Pearson correlation coefficients for indices of area burned and El Niño/Southern Oscillation (ENSO) and Pacific Decadal Oscillation (PDO).

Statistical test	BAI	PC1	PC2	PC3	PC4
$r$ , ENSO†	-0.009	0.272	-0.052	-0.056	0.227
$r$ , PDO†	<b>0.403</b>	<b>0.422</b>	0.018	-0.173	0.125
$t$ test, ENSO‡	0.255	0.275	0.646	0.923	0.740
$t$ test, PDO‡	0.178	<b>0.047</b>	0.652	0.204	0.179

Notes: Statistically significant results ( $\alpha = 0.05$ ) are indicated in boldface type. Key to abbreviations: BAI, burned area index; PC1, principal-components axis 1; PC2, principal-components axis 2, etc.

† Pearson product-moment correlation;  $r \geq 0.25$  is significant at the 95% confidence level. The mean October–March index was used for both the Cold Tongue Index (CTI) and the PDO index.

‡  $P$  value from  $t$  test shown.

there is a modest correlation between PC4 and drought occurrence east of the Cascades crest for the entire year preceding the fire season and between PC4 and reduced drought stress west of the Cascades during the fire season (Fig. 16). This result suggests that summertime cyclones lead to increases in area burned east of the Cascades most commonly when the region is experiencing long-term soil moisture deficits. The increased moisture west of the Cascades is consistent with the hypothesis that summertime cyclones are delivering precipitation only to the coastal region. The forests that load negatively on EOF4 therefore tend to exhibit increases in area burned when the PDSI is negative, a response that is distinct from the relationships seen for PC1. The exception to this finding is Olympic National Forest, which is located in the region characterized by positive correlations to summertime PDSI; increases in area burned therefore correspond to enhanced fire-sea-

son drought. This response is similar to the relationship identified for PC3, but the persistence of the antecedent drought is much shorter. One possible explanation, which cannot be verified by the current analysis, is that this eigenvector is capturing variability at stands within Olympic National Forest that are located in the rain-shadow of the Olympic Mountains and therefore do not require long preceding drought in order to burn.

Correlations between the four PC time series and the CTI and PDO index reveal significant associations only between PC1 and the PDO (Table 2). Furthermore, a difference of means test identified a significant difference in area burned (as represented by PC1) between the warm and cool PDO regimes (Fig. 17). No statistically significant association with ENSO was found for any of the PC time series. These results are consistent with the climatic impacts of the PDO, which are expressed most strongly as reduced wintertime precipitation (Mantua et al. 1997, Gershunov and Barnett 1998, Barlow et al. 2001). PC1 exhibits the strongest and most consistent relationship to drought of the patterns identified here. While PC3 also exhibited good correspondence to drought, the lack of a linear relationship suggests that drought alone is not sufficient to trigger large wildfires.

## CONCLUSIONS

The results presented here provide evidence for a climatic component in forcing extreme wildfire years in the American Northwest. The application of EOF analysis to the area burned record revealed four distinct patterns in area burned; each in turn was related to underlying geographic and ecological factors. Throughout the region, increases in annual area burned are associated with increased 500 hPa heights over western North America and the adjacent North Pacific Ocean. These blocking ridges divert moisture away from the region, raising air temperatures and reducing relative humidity. In extreme cases, this circulation pattern can lead to anomalous easterly “foehn” or “chinook” winds that warm and dry as they descend adiabatically from the continental interior. Prolonged antecedent drought preconditions many of the forests of the region to burn, in

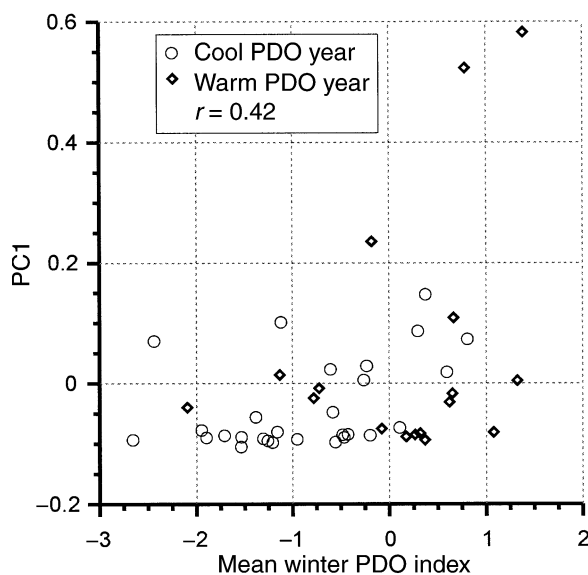


FIG. 17. Scatterplot of leading principal component of area burned (PC1) vs. mean winter (December, January, February) Pacific Decadal Oscillation (PDO) index. Warm PDO phase years (1978–1994) are indicated by diamonds, and cool phase years (1949–1976) are indicated by circles.

particular mesic to wet highly productive forests dominated by Sitka spruce and western hemlock. These forests typically have high fuel loads, but require unusually severe drought to become flammable. The relationship between circulation anomalies and area burned is weakly linear in nature, with particularly large-fire years exhibiting a stronger association to circulation anomalies than either moderate- or small-fire years.

The finding that many of the National Forests respond to similar patterns in atmospheric circulation and drought has implications for the suitability of eigenvector techniques in discriminating true "modes" in area burned, as the patterns in area burned are unlikely to be entirely independent of each other. Furthermore, the linearity assumption of PCA does not appear to be appropriate, as small-fire years are not simply the inverse of large-fire years in their underlying forcing agents or spatial arrangement. Nonorthogonal rotations could potentially overcome some of these limitations, and their suitability for analyses of this type merits further investigation.

The principal findings of this analysis are:

- 1) Years with region-wide increases in area burned are characterized by enhanced drought in the seasons preceding the fire season, followed by continued drought and increases in 500 hPa height over western North America and the eastern Pacific Ocean in the month prior to, throughout, and the month following the normal fire season. The total length of the fire season appears to be a more important determinant of area burned than either the magnitude or persistence of individual fire weather events.

- 2) Distinct ecological characteristics modulate the response to atmospheric forcing, with wetter forests requiring more severe drought and prolonged blocking to burn than drier forests, which may respond to blocking events without antecedent drought.

- 3) The PDO appears to influence wildfire activity, although area burned responds to annual to interannual fluctuations in the PDO more strongly than to interdecadal variability. It is unclear from this analysis whether the PDO influences wildfire activity through its influence on drought severity (i.e., largely a wintertime connection) or by altering the statistics of summertime circulation. No significant association to ENSO was found for any of the records of area burned.

- 4) Eigenvector techniques are able to discriminate distinct patterns in area burned; however, they are probably not the ideal approach to analyze wildfire data in the American Northwest. There are at least three possible explanations for their limited applicability: the record of area burned may be too short and too noisy to resolve meaningful "modes" in forests with long fire return intervals; the patterns in area burned may not be statistically independent from each other; the patterns in area burned are probably not linear in nature, and small-fire years are not simply the inverse of

large-fire years with respect to regional variability in area burned.

In the context of these findings, fire management needs to consider that there are both top-down and bottom-up controls on extreme wildfire years. Although fuel treatments are undoubtedly a necessary component of effective fire management, they cannot realistically be expected to eliminate large area burned in severe fire weather years. Additionally, the potential consequences of impending climate change on fire severity needs greater consideration. The most recent Intergovernmental Panel on Climate Change assessment (IPCC 2001) predicts increased drought stress for the American Northwest, which could lead to more frequent and/or more severe wildfire years in spite of ongoing fuel treatments (McKenzie et al. 2004).

#### ACKNOWLEDGMENTS

This manuscript was greatly improved through discussions with Philip Mote, Jim Agee, Don McKenzie, and an anonymous reviewer. This publication is funded by the Joint Institute for the Study of the Atmosphere and Ocean (JISAO) under NOAA Cooperative Agreement No. NA17RJ1232, contribution #1077. Ze'ev Gedalof is also supported by the Natural Sciences and Engineering Research Council of Canada. David Peterson is supported by the USDA Forest Service. This paper is a contribution from the Western Mountain Initiative.

#### LITERATURE CITED

- Agee, J. K. 1991. Fire history along an elevational gradient in the Siskiyou Mountains, Oregon. *Northwest Science* **65**: 188–199.
- Agee, J. K. 1993. Fire ecology of Pacific Northwest forests. Island Press, Washington, D.C., USA.
- Agee, J. K. 1997. The severe weather wildfire: too hot to handle? *Northwest Science* **71**:153–157.
- Agee, J. K. 1998. The landscape ecology of western forest fire regimes. *Northwest Science* **72**:24–34.
- Agee, J. K., and R. Flewelling. 1983. A fire cycle model based on climate for the Olympic Mountains, Washington. *Fire and Forest Meteorology Conference Proceedings* **7**:32–37.
- Agee, J. K., and M. H. Huff. 1987. Fuel succession in a western hemlock/Douglas-fir forest. *Canadian Journal of Forest Research* **17**:697–704.
- Agee, J. K., and F. Krusemark. 2001. Forest fire regime of the Bull Run watershed, Oregon. *Northwest Science* **75**:292–306.
- Baker, W. L., and D. Ehle. 2001. Uncertainty in surface-fire history: the case of ponderosa pine forests in the western United States. *Canadian Journal of Forest Research* **31**: 1205–1226.
- Barlow, M., S. Nigam, and E. H. Berbery. 2001. ENSO, Pacific decadal variability, and U.S. summertime precipitation, drought, and stream flow. *Journal of Climate* **14**: 2105–2128.
- Bork, J. L. 1984. Fire history in three vegetation types on the eastern side of the Oregon cascades. Dissertation. Oregon State University, Corvallis, Oregon, USA.
- Chen, J., S. C. Saunders, T. R. Crow, R. J. Naiman, K. D. Brosofske, G. D. Mroz, B. L. Brookshire, and J. F. Franklin. 1999. Microclimate in forest ecosystem and landscape ecology. *Bioscience* **49**:288–297.
- Countryman, C. M., M. H. McCutchan, and B. C. Ryan. 1969. Fire weather and fire behavior at the 1968 Canyon fire. Research Paper PSW-55. USDA Forest Service, Berkeley, California, USA.
- Cwynar, L. C. 1987. Fire and the forest history of the North Cascade range. *Ecology* **68**:791–802.

- Everett, R. L., R. Schellhaas, D. Keenum, D. Spurbeck, and P. Ohlson. 2000. Fire history in the ponderosa pine/Douglas-fir forests on the east slope of the Washington Cascades. *Forest Ecology and Management* **129**:207–225.
- Fahnestock, G. R., and J. K. Agee. 1983. Biomass consumption and smoke production by prehistoric and modern forest fires in western Washington. *Journal of Forestry* **81**:653–657.
- Finklin, A. I. 1973. Meteorological factors in the Sundance fire run. General Technical Report INT-6. USDA Forest Service, Ogden, Utah, USA.
- Flannigan, M. D., and J. B. Harrington. 1988. A study of the relation of meteorological variables to monthly provincial area burned by wildfire in Canada (1953–1980). *Journal of Applied Meteorology* **27**:441–452.
- Franklin, J. F., and C. T. Dyrness. 1973. Natural vegetation of Oregon and Washington. Forest Service, U.S. Department of Agriculture, Portland, Oregon, USA.
- Gauch, H. G. 1980. Noise reduction by eigenvector ordinations. *Ecology* **63**:1643–1649.
- Gavin, D. G., L. B. Brubaker, and K. P. Lertzman. 2003a. An 1800-year record of the spatial and temporal distribution of fire from the west coast of Vancouver Island, Canada. *Canadian Journal of Forest Research* **33**:573–586.
- Gavin, D. G., L. B. Brubaker, and K. P. Lertzman. 2003b. Holocene fire history of a coastal temperate rainforest based on soil charcoal radiocarbon dates. *Ecology* **84**:186–201.
- Gedalof, Z., and D. J. Smith. 2001. Interdecadal climate variability and regime-scale shifts in Pacific North America. *Geophysical Research Letters* **28**:1515–1518.
- Gershunov, A., and T. P. Barnett. 1998. Interdecadal modulation of ENSO teleconnections. *Bulletin of the American Meteorological Society* **79**:2715–2725.
- Guttman, N. B., and R. G. Quayle. 1996. A historical perspective of U.S. climate divisions. *Bulletin of the American Meteorological Society* **77**:293–303.
- Hare, S. R., and N. J. Mantua. 2000. Empirical evidence for North Pacific regime shifts in 1977 and 1989. *Progress in Oceanography* **47**:103–146.
- Hessburg, P. F., B. G. Smith, R. B. Salter, R. D. Ottmar, and E. Alvarado. 2000. Recent changes (1930s–1990s) in spatial patterns of interior northwest forests, USA. *Forest Ecology and Management* **136**.
- Huff, M. H. 1995. Forest age structure and development following wildfires in the western Olympic Mountains, Washington. *Ecological Applications* **5**:471–483.
- IPCC [Intergovernmental Panel on Climate Change]. 2001. Climate change 2001: impacts, adaptation and vulnerability. In J. J. McCarthy, O. F. Canziani, N. A. Leary, D. J. Dokken, and K. S. White, editors. Contribution of Working Group II to the Third Assessment Report of the Intergovernmental Panel on Climate Change. Cambridge University Press, Cambridge, UK.
- Jackson, P. L., and A. J. Kimerling, editors. 1993. Atlas of the Pacific Northwest. Eighth edition. Oregon State University Press, Corvallis, Oregon, USA.
- Johnson, E. A. 1992. Fire and vegetation dynamics: studies from the North American boreal forest. Cambridge University Press, Cambridge, UK.
- Johnson, E. A., K. Miyanishi, and S. R. J. Bridge. 2001. Wildfire regime in the boreal forest and the idea of suppression and fuel buildup. *Conservation Biology* **15**:1554–1557.
- Johnson, E. A., and D. R. Wowchuk. 1993. Wildfires in the southern Canadian Rocky Mountains and their relationship to mid-tropospheric anomalies. *Canadian Journal of Forest Research* **23**:1213–1222.
- Kalnay, E., et al. 1996. The NCEP/NCAR 40-year reanalysis project. *Bulletin of the American Meteorological Society* **77**:437–471.
- Knox, J. L., and R. G. Lawford. 1990. The relationship between Canadian Prairie dry and wet months and circulation anomalies in the mid troposphere. *Atmosphere-Ocean* **28**:189–215.
- Kumar, A., and M. P. Hoerling. 1998. Annual cycle of Pacific-North American seasonal predictability associated with different phases of ENSO. *Journal of Climate* **11**:3295–3308.
- Lertzman, K., J. Fall, and B. Dorner. 1998. Three kinds of heterogeneity in fire regimes: at the crossroads of fire history and landscape ecology. *Northwest Science* **72**:4–23.
- Li, C. 2002. Estimation of fire frequency and fire cycle: a computational perspective. *Ecological Modelling* **154**:103–120.
- Mantua, N. J., S. R. Hare, Y. Zhang, J. M. Wallace, and R. C. Francis. 1997. A Pacific interdecadal climate oscillation with impacts on salmon production. *Bulletin of the American Meteorological Society* **78**:1069–1079.
- McKenzie, D., Z. Gedalof, D. L. Peterson, and P. Mote. 2004. Climatic change, wildfire, and conservation. *Conservation Biology* **18**:890–902.
- North, G. R., T. L. Bell, R. F. Cahalan, and F. J. Moeng. 1982. Sampling errors in the estimation of empirical orthogonal functions. *Monthly Weather Review* **110**:699–706.
- Ropelewski, C. F., and M. S. Halpert. 1986. North American precipitation and temperature patterns associated with the El Niño/Southern Oscillation (ENSO). *Monthly Weather Review* **114**:2352–2362.
- Sando, R. W., and D. A. Haines. 1972. Fire weather and behavior of the Little Sioux fire. Research Paper NC-76. USDA Forest Service, St. Paul, Minnesota, USA.
- Schroeder, M. J. 1969. Critical fire weather patterns in the conterminous United States. Technical Report WB 8. Weather Bureau, U.S. Department of Commerce, Environmental Science Services Administration, Silver Spring, Maryland, USA.
- Skinner, W. R., M. D. Flannigan, B. J. Stocks, D. L. Martell, B. M. Wotton, J. B. Todd, J. A. Mason, K. A. Logan, and E. M. Bosch. 2002. A 500 hPa synoptic wildland fire climatology for large Canadian forest fires, 1959–1996. *Theoretical and Applied Climatology* **71**:157–169.
- Skinner, W. R., B. J. Stocks, D. L. Martell, B. Bonsal, and A. Shabbar. 1999. The association between circulation anomalies in the mid-troposphere and area burned by wildfire in Canada. *Theoretical and Applied Climatology* **63**:89–105.
- Strauss, D., L. Bednar, and R. Mees. 1989. Do one percent of forest fires cause ninety-nine percent of the damage? *Forest Science* **35**:319–328.
- Street, R. B., and M. E. Alexander. 1980. Synoptic weather associated with five major forest fires in Pukaskwa National Park. Reg. Int. Rep. SSD-80-2. Atmosphere Environment Service, Toronto, Ontario, Canada.
- Street, R. B., and E. C. Birch. 1986. Synoptic fire climatology of the Lake Athabasca–Great Slave Lake Area, 1977–1982. *Climatological Bulletin* **21**:3–25.
- Taylor, A. H., and C. N. Skinner. 1998. Fire history and landscape dynamics in a late-successional reserve, Klamath Mountains, California, USA. *Forest Ecology and Management* **111**:285–301.
- Trenberth, K. E., and J. W. Hurrell. 1994. Decadal atmosphere–ocean variations in the Pacific. *Climate Dynamics* **9**:303–319.
- Weaver, H. 1959. Ecological changes in the ponderosa pine forest of the Warm Springs Indian Reservation in Oregon. *Journal of Forestry* **57**:15–20.
- Westerling, A. L., A. Gershunov, T. J. Brown, D. R. Cayan, and M. D. Dettinger. 2003. Climate and wildfire in the western United States. *Bulletin of the American Meteorological Society* **84**:595–604.
- Yarnal, B., and H. F. Diaz. 1986. Relationships between extremes of the Southern Oscillation and the winter climate of the Anglo-American Pacific coast. *Journal of Climatology* **6**:197–219.
- Zhang, Y., J. M. Wallace, and D. Battisti. 1997. ENSO-like interdecadal variability: 1900–93. *Journal of Climate* **10**:1004–1020.